Title	Architectural design and load flow study of power flow routers
Author(s)	Lin, J; Li, VOK; Leung, KC; Lam, AYS
Citation	The 5th IEEE International Conference on Smart Grid Communications (SmartGridComm 2014), Venice, Italy, 3-6 November 2014. In Conference Proceedings, 2014, p. 37-42
Issued Date	2014
URL	http://hdl.handle.net/10722/201225
Rights	IEEE International Conference on Smart Grid Communications (SmartGridComm) Proceedings. Copyright © IEEE.

Architectural Design and Load Flow Study of Power Flow Routers

Junhao Lin, Victor O. K. Li, Ka-Cheong Leung
Department of Electrical and Electronic Engineering
The University of Hong Kong
Email: {jhlin, vli, kcleung}@eee.hku.hk

Albert Y. S. Lam
Department of Computer Science
Hong Kong Baptist University
Email: albertlam@ieee.org

***Abstract*—Power flow routing is an emerging control paradigm for the dynamic and responsive control of electric power flows. In this paper, we investigate the design and modelling of the power flow router (PFR) which is a major building block of power flow routing. First, a generic PFR architecture is proposed to encapsulate the desired functions of PFRs. Then, the load flow model of PFRs is developed and incorporated into the optimal power flow (OPF) framework. Based on the load flow model, the control capabilities of PFR, such as decoupled branch power flows and enlarged flow regions, are analysed. With particular attention to available transfer capability (ATC), an OPF study on the standard IEEE benchmark systems with 14, 57, and 118 buses has been performed to show that ATC can be enhanced remarkably by installing the proposed PFRs at some critical buses of the power network.**

I. Introduction

The rapid increase in energy demand and the integration of renewable energy sources (RESs) [1] are stressing the power grid, prompting system operators to take active control measures for managing the power flow more efficiently and intelligently. Power flow routing [2], an emerging control paradigm evolved from the traditional power flow control, is a promising solution due to the development of power electronics over the past two decades [3], [4].

Power flow controllers (PFCs) and power flow routers (PFRs) are the building blocks of power flow routing. The literature usually does not make a clear distinction between PFCs and PFRs. In this paper, in order to avoid ambiguity, we use PFR to refer to a control device that is able to manage multiple incoming/outgoing power flows, and PFC to refer to a device that can only actively adjust the power flow through one transmission line or appliance. Hence, a PFC is one part of a PFR. The most popular PFCs are flexible alternating current transmission system (FACTS) devices [3], such as unified power flow controller (UPFC) and static synchronous compensator (STATCOM), which have been adopted for improving asset utilization [5].

The need for a smarter and more resilient grid has led to continuous innovations on PFCs [6], [7] and PFRs [8]–[10]. Most research efforts have been devoted to the hardware implementation of PFCs and PFRs [6], [7], [9], [10], and we have found only one paper [8] focusing on a generic architecture of a PFR. However, the PFR model proposed in [8] is just a simple combination of a computational unit and several PFCs, and only applicable to the distribution network. The lack of a generic functional model of PFRs has hindered network-level research on power flow routing. To resolve this situation, we propose a generic PFR model that covers the necessary and desired functions of a PFR so as to facilitate the theoretical study of power flow routing.

The load flow model of a PFR should also be developed for power flow analysis. However, existing work on load flow modelling for PFRs is limited, although the research on load flow models of PFCs is rich [3], [11]. A sensitivity method is employed in [11] to analyse the impact of PFCs on corrective power flow control. However, due to the inherent complexity of the method, power losses and the reactive power are not considered in [11]. In this paper, we develop a rigorous PFR load flow model characterized by "branch terminal voltages." We show that the proposed load flow model provides a direct and convenient way to analyse the flow control region of a PFR. More importantly, the optimal power flow (OPF) problem incorporating the proposed load flow model of PFRs can also be solved efficiently and optimally by the exact convex relaxation inspired by the methods proposed in [12], [13]. Available transfer capability (ATC) [5] is chosen to assess the efficacy of our PFR model since ATC is an important factor in accommodating demand and RES.

To summarise, we propose a generic architecture and a load flow model of PFRs, and study the enhancement of ATC by introducing the proposed PFR model into the power network. The contributions of this paper are as follows:

- The proposed architecture encapsulates the desired features of PFRs, and is amenable for implementation as well as for the theoretical study of power flow routing.
- The proposed load flow model captures the operating principle of PFRs and the physics of power flows, and is useful for analysing the flow control region of PFRs.
- We present a method to incorporate PFR into the OPF model and convexify this revised OPF. A placement algorithm is applied to investigate the relationship between the ATC improvement and the number of PFRs available in the power network.

II. Generic Architecture of Power Flow Routers

A PFR should manage all of its incoming/outgoing power flows intelligently, and coordinate with other grid participants

to maintain the system stability. Therefore, the following functions are desired for a PFR:

- autonomous control and coordination of multiple incoming/outgoing power flows;
- independent control of active and reactive power flows for each branch;
- various types of interfaces to support alternating current (AC) or direct current (DC) power flows at different voltage and power levels;
- voltage regulation and reactive power compensation; and
- power buffering and energy storage.

Based on the design objectives above, we propose a generic architecture of a PFR as shown in Fig. 1. Existing PFRs [8]–[10] can be viewed as some particular embodiments of the proposed architecture. PFR replaces the conventional bus. Two major types of power flows, namely, branch power flows from/to other PFRs/buses, and local power injections, are connected to a PFR. Within the PFR, all power flows share a "common bus" after flowing through the respective PFCs or interfaces. Meanwhile, the control capabilities of PFCs enable the autonomous control of the corresponding power flows.

The common bus of the PFR should be distinguished from the conventional bus in the power network. It can be an AC or DC bus, depending on the implementation. The branch flow should go through a "line PFC" before connecting to the common bus. The line PFC controls the active and reactive power flows of its connected external transmission line. For example, distribution system PFRs [8], [10] usually have DC common buses and AC/DC converters as line PFCs. As for the transmission system PFR, the UPFC [3] or the controllable network transformer (CNT) [6] can be a line PFC if an AC common bus is used.

The local power injections are categorised into five types, namely, energy storage, dispatchable generation, intermittent RES, critical load, and elastic load. Energy storage acts as the buffer for a PFR. The intermittent RES power would go through a so-called RES PFC before reaching the common bus. RES PFC is for regulating the RES power, such as reactive power compensation and voltage regulation. Local demand is classified into the critical load which has to be met in real time, and the elastic load which may be a deferrable load or a noncritical load that can withstand power fluctuations. The load PFC between the common bus and the elastic load can be an electric spring [14] to regulate the common bus voltage and absorb the fluctuations of the RES power.

The operations of the PFCs and interfaces are coordinated by a central processing unit (CPU) which is the central controller of the PFR. PFRs would also communicate and coordinate with each other via their central controllers in the power network.

It should be noted that the architecture in Fig. 1 is a complete and ideal configuration of a PFR. A practical PFR may sacrifice certain power flow control capability to strike a balance between the control capacity and the costs for the devices.

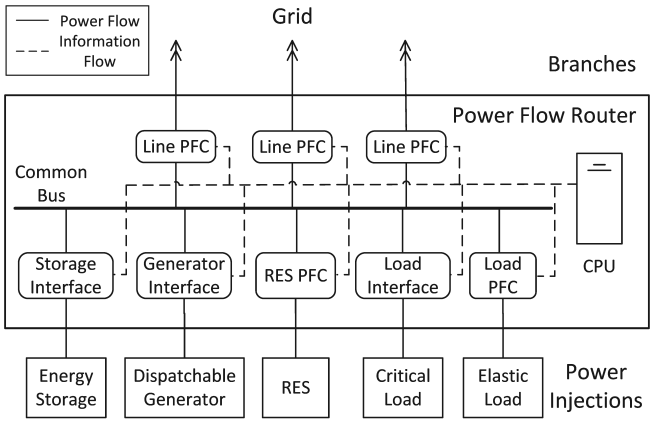

Fig. 1. Proposed architecture of a power flow router.

III. Load Flow Model and Optimal Power Flow

A. Load Flow Model of PFR

The load flow model of a PFR will be developed based on the architecture proposed in Section II. Consider a power network with the bus set $\mathcal{N} := \{1, 2, \ldots, N\}$ and the set of transmission lines $\mathcal{E} \subseteq \mathcal{N} \times \mathcal{N}$. A branch or transmission line $(i, j) \in \mathcal{E}$ with its two terminal buses $i, j \in \mathcal{N}$ is modelled by the equivalent π circuit with the line admittance $y_{ij} = g_{ij} + \mathrm{j}b_{ij}$, where $g_{ij} > 0$ and $b_{ij} < 0$ denote the conductance and susceptance of branch (i, j), respectively, and the shunt capacitance $c_{ij} = c_{ji}$ as illustrated in Fig. 2. Denote the set of one-hop connected neighbours of a bus $i \in \mathcal{N}$ as $\Omega_i \subseteq \mathcal{N}$.

Denote the PFR installed at a bus $i \in \mathcal{N}$ as PFR i. The branch power flows and the local power injections of bus i are interfaced to PFR i. The common bus of PFR i is characterized by the voltage phasor V_i analogous to that of a conventional bus. Furthermore, for each one-hop connected bus/PFR $j \in \Omega_i$ of PFR i, there is a "branch terminal voltage" $V_{i_j} \in \mathbb{C}$, indicating the output voltage of PFR i for branch (i, j). In other words, for every branch $(i, j) \in \mathcal{E}$, there are two corresponding branch terminal voltages, namely, V_{i_j} and V_{j_i}, as illustrated in Fig. 2. The operating range of the branch terminal voltage V_{i_j} follows (1).

$$\begin{cases} \left|V_{i_j} - V_i\right| \le \gamma_{i_j,max} \left|V_i\right|, & \text{for PFR } i \text{ with AC common bus} \\ U_{i_j,min} \le \left|V_{i_j}\right| \le U_{i_j,max}, & \text{for PFR } i \text{ with DC common bus} \end{cases} \tag{1}$$

From (1), for an AC common bus, the line PFC can be modelled as a series voltage injection [3], [7] and $\gamma_{i_j,max} \in [0, 1]$ characterizes the capability of voltage control of the line PFR. For a DC common bus, the line PFC can be modelled

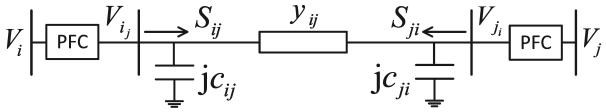

Fig. 2. Notations for a branch (i, j).

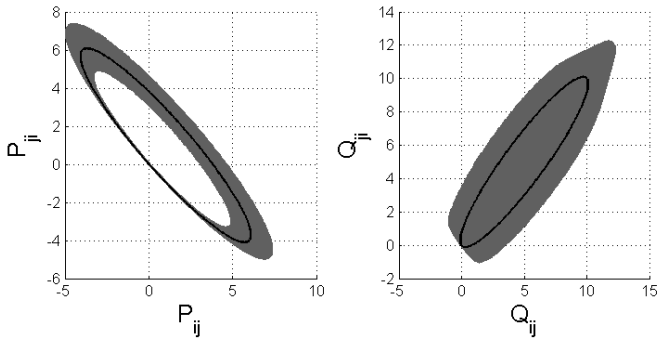

Fig. 3. Active and reactive power flow regions of a branch. The black ellipses are the curves when no PFC or PFR is available. The shaded areas are the flow regions when PFRs are equipped in the two buses.

as an AC/DC converter and $U_{i_j,min}, U_{i_j,max} > 0$ specifies the control region of the branch terminal voltage V_{i_j}. In addition, the PFC, as a power electronic device, of PFR i in branch (i,j) might possess certain extra capability of reactive power compensation which is modelled by the reactive power injection Q_{Cij}.

Let P_i and Q_i denote the aggregate local power injection for active and reactive powers, respectively, of PFR i. Then, the power balance equation for PFR i is formulated as:

$$P_i + \mathrm{j}Q_i = \sum_{j\in\Omega_i} \left(V_{i_j}(V_{i_j} - V_{j_i})^* y_{ij}^* - \frac{\mathrm{j}}{2} \left|V_{i_j}\right|^2 c_{ij} + \mathrm{j}Q_{Cij} \right) \quad (2)$$

where * denotes the conjugate operator of a complex number.

A branch power flow is controlled by the terminal voltages of the two buses/PFRs on both ends. As implied in (1), for the case of V_i with any fixed magnitude, each branch terminal voltage $\{V_{i_j} | j \in \Omega_i\}$ of a PFR $i \in \mathcal{N}$ can be controlled independently by the corresponding line PFC. Therefore, the PFR can achieve decoupled control of its branch power flows.

Consider the power flow regions of branch (i,j) in Fig. 2. Assume that $|V_i| = |V_j| = 1$ p.u., $y_{ij} = (1 - 5\mathrm{j})$ p.u., and $c_{ij} = 0$. Without any PFC or PFR, similar to [15], the active power flows (P_{ij}, P_{ji}) and the reactive power flows (Q_{ij}, Q_{ji}) of (S_{ij}, S_{ji}) form two respective ellipses plotted in black curves in Fig. 3. When a PFR with an AC common bus is installed at each of the two buses with $\gamma_{i_j,max} = \gamma_{j_i,max} = 0.1$ in (1), the flow regions of (P_{ij}, P_{ji}) and (Q_{ij}, Q_{ji}) are enlarged to the two respective shaded areas in Fig. 3. The enlarged control regions contribute to the reduction of power losses, improvement of power transfer capability, and of reactive power compensation.

B. PFR-Incorporated Optimal Power Flow

The load flow model of the PFR developed in Section III-A will be incorporated into the OPF problem. The PFR-enabled OPF is different from the traditional OPF since the voltage of a bus without PFR has evolved into several autonomous branch terminal voltages when the PFR is applied to the bus. Therefore, the matrix of voltage phasors, $\mathbf{V} \in \mathbb{C}^{N\times N}$, is defined in (3) to represent all the branch terminal voltages of PFRs in the power network.

$$[\mathbf{V}]_{i,j} := \begin{cases} V_{i_j} & (i,j) \in \mathcal{E} \\ 0 & (i,j) \notin \mathcal{E} \end{cases} \quad (3)$$

Similarly, define the line admittance matrix $\mathbf{Y} \in \mathbb{C}^{N\times N}$ by $[\mathbf{Y}]_{i,j} := y_{ij}$ and the shunt capacitance matrix $\mathbf{C} \in \mathbb{R}^{N\times N}$ by $[\mathbf{C}]_{i,j} := c_{ij}$, for $(i,j) \in \mathcal{E}$. The entries of $\mathbf{Y}$ and $\mathbf{C}$ are zeros for those elements with $(i,j) \notin \mathcal{E}$.

We minimize a global objective function f of the power network, subject to the power balance constraints at PFRs/buses, the constraints for the control regions of PFRs, and the constraints for branch power flows. The general form of the PFR-incorporated OPF (PFR-OPF) is formulated as follows:

$$\min f \quad (4a)$$

subject to

$$\mathbf{P} + \mathrm{j}\mathbf{Q} = \mathrm{diag}\big(\mathbf{V}((\mathbf{V} - \mathbf{V}^T) \circ \mathbf{Y} + \mathrm{j}\mathbf{V} \circ \mathbf{C})^H\big) + \mathrm{j}\mathbf{Q_C} \quad (4b)$$

$$U_{i,min} \le |V_i| \le U_{i,max}, \forall i \in \mathcal{N} \quad (4c)$$

(1) holds $\forall (i,j) \in \mathcal{E}$ (4d)

$$\left| V_{i_j}(V_{i_j} - V_{j_i})^* y_{ij}^* - \frac{\mathrm{j}}{2}|V_{i_j}|^2 c_{ij} \right| \le S_{ij,max}, \forall (i,j) \in \mathcal{E} \quad (4e)$$

$$Q_{Cij,min} \le Q_{Cij} \le Q_{Cij,max}, \forall (i,j) \in \mathcal{E} \quad (4f)$$

From (4b), $\mathbf{P}, \mathbf{Q} \in \mathbb{R}^N$ are the vectors for the aggregate active and reactive power injections, respectively. $\mathbf{Q_C} \in \mathbb{R}^N$ is defined by $[\mathbf{Q_C}]_i = \sum_{j\in\Omega_i} Q_{Cij}$. The function $\mathrm{diag}(\mathbf{A})$ is for extracting the diagonal elements of an arbitrary square matrix $\mathbf{A}$ and forming the diagonal elements into a vector. $\circ$ denotes the operator of the Hadamard product. H denotes the conjugate transpose operator of a matrix.

C. PFR-OPF for Available Transfer Capability

ATC is one of the key indicators for the reliable operation of power systems. According to [5], ATC is assessed by increasing all of the loads by a loading factor $\lambda \ge 0$ until the system reaches the critical state. Therefore, extended from the general PFR-OPF in (4), the PFR-OPF for ATC can be formulated in (5) as follows:

$$\min_{\mathbf{V},\mathbf{P_G},\mathbf{Q_G},\mathbf{P_L},\mathbf{Q_L},\{V_i|i\in\mathcal{N}\},\lambda} -\sum_{i\in\mathcal{N}} P_{Li} + \alpha P_{loss} \quad (5a)$$

subject to

$$\mathbf{P} + \mathrm{j}\mathbf{Q} = (\mathbf{P_G} - \mathbf{P_L}) + \mathrm{j}(\mathbf{Q_G} - \mathbf{Q_L}) \quad (5b)$$

$$P_{Li} = \lambda P_{Li0}, \forall i \in \mathcal{N} \quad (5c)$$

$$Q_{Li} = \lambda Q_{Li0}, \forall i \in \mathcal{N} \quad (5d)$$

$$P_{Gi,min} \le P_{Gi} \le P_{Gi,max}, \forall i \in \mathcal{N} \quad (5e)$$

$$Q_{Gi,min} \le Q_{Gi} \le Q_{Gi,max}, \forall i \in \mathcal{N} \quad (5f)$$

and (4b), (4c), (4d), (4e), (4f)

The general PFR-OPF formulation in (4) has not specified the operating range for local power injections. For this particular problem on ATC assessment (5), the local power injections are categorised into the dispatchable generation and critical load as indicated in (5b). From (5b), $\mathbf{P_G}, \mathbf{Q_G} \in \mathbb{R}^N$ denote

the vectors of active and reactive generations, respectively. $\mathbf{P_L}, \mathbf{Q_L} \in \mathbb{R}^N$ denote the vectors of active and reactive loads, respectively. $\alpha \in (0, 1]$ is a preset coefficient and P_{loss} represents the active power losses of the entire network determined as follows:

$$P_{loss} := \sum_{i \in \mathcal{N}} \sum_{j \in \Omega_i} \text{Re}\left\{V_{i_j} \left(V_{i_j} - V_{j_i}\right)^* y_{ij}^*\right\} \tag{6}$$

The inclusion of the adjustment term αP_{loss} in the objective function of (5) is to avoid excessive active power losses of the network. From (5c) and (5d), $P_{Li0} \geq 0$ and $Q_{Li0} \in \mathbb{R}$ are the base active and reactive loads, respectively, of Bus/PFR i. Denote the optimal loading factor as λ^{opt} obtained by solving the PFR-OPF problem in (5). Then, ATC is given as follows:

$$ATC := \left(\lambda^{opt} - 1\right) \sum_{i \in \mathcal{N}} P_{Li0} \tag{7}$$

IV. Convex Relaxation and Placement Algorithm

A. Convex Relaxation of PFR-OPF for ATC

Inspired by the methods for convexifying the OPF problem presented in [12], [13], the proposed PFR-OPF for ATC in (5) is reformulated as a second-order cone programming (SOCP) problem. Two auxiliary variables $\mathbf{M} \in \mathbb{R}^{N \times N}$ and $\mathbf{W} \in \mathbb{C}^{N \times N}$ are introduced as:

$$[\mathbf{M}]_{i,j} := V_{i_j} V_{i_j}^* \tag{8}$$

$$[\mathbf{W}]_{i,j} := V_{i_j} V_{j_i}^* \tag{9}$$

The convexified PFR-OPF for ATC is formulated as follows:

$$\min_{\mathbf{M}, \mathbf{W}, \mathbf{P_G}, \mathbf{Q_G}, \mathbf{P_L}, \mathbf{Q_L}, \{V_i | i \in \mathcal{N}\}, \lambda} - \sum_{i \in \mathcal{N}} P_{Li} + \alpha P_{loss} \tag{10a}$$

subject to

$$\mathbf{P} + \mathrm{j}\mathbf{Q} = \text{diag}\left((\mathbf{M} - \mathbf{W})\mathbf{Y}^H + \mathbf{M}\mathbf{C}^H\right) + \mathrm{j}\mathbf{Q_C} \tag{10b}$$

$$[\mathbf{M}]_{i,j}[\mathbf{M}]_{j,i} \geq [\mathbf{W}]_{i,j}[\mathbf{W}]_{j,i}, \forall (i,j) \in \mathcal{E} \tag{10c}$$

and (4c) – (4f), (5b) – (5f)

Assumption 1. *The constraint*

$$\left|\angle V_{i_j} - \angle V_{j_i}\right| \leq \arctan -\frac{b_{ij}}{g_{ij}}, \forall (i,j) \in \mathcal{E} \tag{11}$$

for the angle difference over a transmission line holds for the PFR-OPF problems in (5) *and* (10)*.*

Assumption 2. *The PFR-OPF problem in* (5) *is feasible.*

Assumption 3. *At least one phase shifter is available for every loop of the power network.*

Theorem 1. *Under Assumptions 1, 2, and 3, the optimal solution of the convexified PFR-OPF problem in* (10) *is exactly the same as that of the original non-convex PFR-OPF problem in* (5)*.*

Sketch of Proof: The PFR possesses the same phase shifting capability as the phase shifter. Therefore, according to [13], under Assumptions 1, 2, and 3, the OPF problem can be relaxed exactly and tightly, i.e., the relaxation retains the same optimal solution of the original problem, as an SOCP problem, if all the PFRs only act as phase shifters, i.e., the voltage magnitude control of PFRs is disabled.

Moreover, a PFR decouples the bus voltage control into independent control of several branch terminal voltages. Therefore, the SOCP relaxation of the second-order terms of branch terminal voltages, indicated by (10c), preserves the same Pareto optimality as that of the SOCP relaxation on bus voltages applied in [13]. In other words, the convexified PFR-OPF problem in (10) is still exact and tight when the voltage magnitude control of the PFR is enabled. ■

B. PFR Placement for ATC Enhancement

In order to investigate the relationship between the ATC enhancement and the number of PFRs required in the network, a PFR placement problem for the ATC enhancement is defined as follows.

Problem 1. *Given a set of PFRs, each of which is labeled by $r_k, k = 1, 2, \ldots, N_R$ where $N_R \leq N$. Each r_k determines the bus b_k that is assigned with PFR r_k, so that the optimal loading factor λ^{opt} obtained is maximized by solving the PFR-OPF problem for ATC in* (5)*.*

It is not difficult to show that Problem 1 is non-deterministic polynomial-time hard.

Under Assumptions 1, 2 and 3, a greedy algorithm, namely, Algorithm 1, is applied to obtain a sub-optimal solution of Problem 1.

Algorithm 1 PFR Placement for ATC Enhancement

Input: The specifications of the PFRs, labeled by $r_k, k = 1, 2, \ldots, N_R$, to be installed in the power network, and other necessary specifications of the power network required by the convexified PFR-OPF problem in (10).

Output: For each PFR $r_k, k = 1, 2, \ldots, N_R$, the bus b_k that is assigned to be installed with the PFR r_k.

Initialize the set of the PFRs that have not been assigned to any bus as $\mathcal{R}_{un} = \{r_k | 1 \leq k \leq N_R\}$, and the set of the buses that have installed PFRs as $\mathcal{B}_R = \emptyset$.

Repeat Steps 1–5 until $\mathcal{R}_{un} = \emptyset$.

1) Pick one PFR $r_m \in \mathcal{R}_{un}$.
2) For each bus $i \in \mathcal{N} \backslash \mathcal{B}_R$, obtain the optimal loading factor λ_i^{opt} by solving the PFR-OPF problem in (10) assuming that PFR r_m is installed at Bus i.
3) Set $b_m \leftarrow \arg\max_{i \in \mathcal{N} \backslash \mathcal{B}_R} \lambda_i^{opt}$, where PFR r_m is assigned to Bus b_m with the largest ATC enhancement.
4) Set $\mathcal{B}_R \leftarrow \mathcal{B}_R \cup \{b_m\}$ and $\mathcal{R}_{un} \leftarrow \mathcal{R}_{un} \backslash \{r_m\}$.
5) If $\mathcal{R}_{un} \neq \emptyset$, go to Step 1.

Return b_k, where $k = 1, 2, \ldots, N_R$.

V. Case Study

In this section, a comprehensive numerical study is performed to investigate the benefits of power flow routing and PFR integration in terms of the ATC enhancement of the power system.

A. Scenarios for Comparison

Three versions of OPF, namely, the traditional OPF (T-OPF) without PFR, the convexified OPF with phase shifters (PS-OPF) [13], and the proposed convexified PFR-OPF in (10) are compared in terms of the network ATC. The utilization of generation capacities, and the network reliability under the $(n-1)$ contingency for an outage of one transmission line, will be tested.

For PFR-OPF, the effect of various configurations of PFRs, i.e., the extra capability of reactive power compensation, and the number of PFRs available in the network, would be investigated.

B. Performance Metric

The performance is evaluated by ATC as presented in (7). According to (7), a larger optimal loading factor λ^{opt} indicates a larger ATC and hence a better performance.

C. General Setup

A numerical study is performed on the standard IEEE benchmark systems with 14, 57, and 118 buses. The parameter specifications of the three tested systems follow the standard settings archived at [16], except for the branch flow limits which are not given in [16]. The branch flow limits of the three tested systems are specified in Table I based on the nominal settings. The per-unit base is 100 MVA in this study.

The impact of the generation capacity on ATC is studied. An index for the generation capacity, I_G, is defined as the generation capacity equal to I_G times of the nominal setting of the capacity of each generator.

In this study, all PFRs are assumed to be configured with AC common buses. For all PFRs, $r_{i_j,max}$ in (1) are set to be 0.1, which is a typical setting for the line PFC [3]. The limits of the branch reactive power compensation are characterized by $Q_L \geq 0$ and set as $Q_{Cij,max} = -Q_{Cij,min} = Q_L$ for all PFRs. The coefficient α in (10a) is set to 0.1.

TABLE I
SPECIFICATIONS OF BRANCH FLOW LIMITS

Branch Type	n-bus system		
	$n=14$	$n=57$	$n=118$
Connected to generator(s)	2.0 p.u.	3.0 p.u.	5.0 p.u.
Not connected to any generator	1.0 p.u.	1.5 p.u.	2.5 p.u.

TABLE II
ATC OF IEEE 14, 57, AND 118-BUS SYSTEMS IN VARIOUS SCENARIOS

OPF	I_G	Q_L (p.u.)	14-Bus		57-Bus		118-Bus	
			λ^{opt}	ATC (MW)	λ^{opt}	ATC (MW)	λ^{opt}	ATC (MW)
T-OPF	1	-	1.952	246.6	1.039	48.78	1.939	3983
	1.5		2.315	340.6	1.040	50.03	2.281	5434
PS-OPF	1	-	2.126	291.7	1.042	52.65	1.944	4004
	1.5		2.442	373.4	1.042	52.88	2.294	5489
PFR-OPF	1	0	2.513	392.0	1.546	682.6	2.285	5449
	1	0.1	2.869	**483.9**	1.550	**687.5**	2.289	**5467**
	1.5	0	3.121	549.4	2.291	1615	3.300	9757
	1.5	0.1	3.892	**748.9**	2.230	**1624**	3.314	**9816**

D. Numerical Results

Table II summarizes the ATC assessment results of the three tested systems over various scenarios, where the results for the proposed PFR-OPF in (10) correspond to full coverage of PFRs, i.e., each bus of the system is equipped with a PFR. It can be observed that the ATCs obtained by the OPF with phase shifters (PS-OPF) are slightly greater than those obtained by the traditional OPF (T-OPF), since the constraint for the angle difference of a loop is relaxed in PS-OPF [13].

By introducing PFRs to the three tested systems, ATCs are improved remarkably as shown in Table II. By comparing the base cases when $I_G = 1$ and the cases when $I_G = 1.5$, the ATC assessment results indicate that the systems with PFRs utilize the increased generation capacities much better than the systems without PFRs. It implies that PFRs can help control and redistribute power flows of the network in a more efficient manner. Moreover, by comparing the results when Q_L equals to 0 or 0.1 p.u., it can be observed that the extra capability of reactive power compensations of PFRs can contribute to the ATC enhancement to a certain extent, although the benefit becomes small as the scale of the system increases.

Fig. 4 presents the network loadability of the IEEE 57-bus system under the $(n-1)$ contingency for an outage of one transmission line when $I_G = 1$. On the one hand, the results of PS-OPF indicate that, when no PFR is available, the network is fragile and sensitive to the transmission line outage. There is frequent occurrence of the optimal loading factor $\lambda^{opt} < 1$, corresponding to when the system cannot even support the base load. On the other hand, in the cases of full coverage of PFRs, the network is resilient and reliable against line outages. Moreover, the extra capability of the reactive power compensation with PFRs introduces a higher reliability to the system, as the loadability remains very stable in the scenario with $Q_L = 0.1$ p.u., while the optimal loading factor falls in some of the cases when $Q_L = 0$.

Fig. 5 presents the PFR placement results of the three tested systems obtained by Algorithm 1. For each scenario, PFRs are added to the network until ATC reaches 99% of the best-possible ATC for this scenario, i.e., the ATC shown in Table

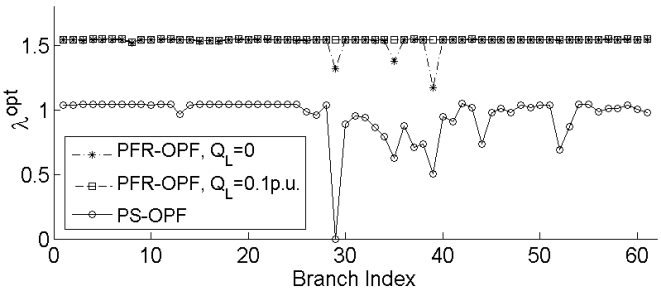

Fig. 4. Network loadability of the IEEE 57-bus system under the $(n-1)$ contingency for an outage of one transmission line.

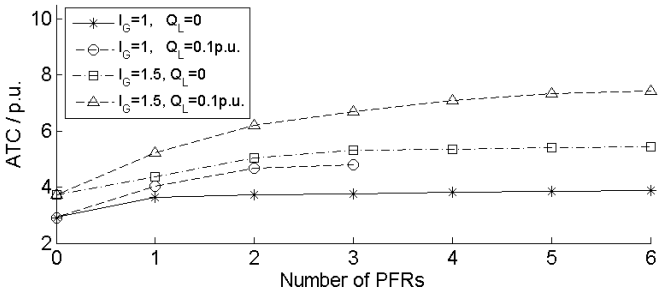

(a) PFR placement results of the IEEE 14-bus system.

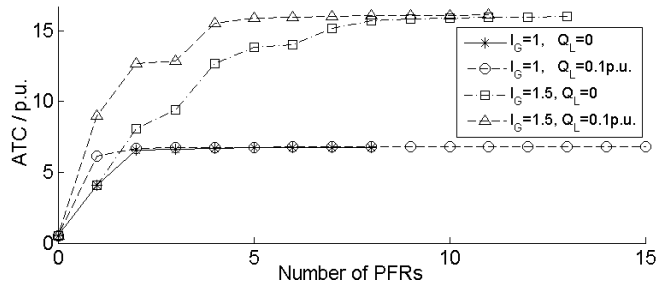

(b) PFR placement results of the IEEE 57-bus system.

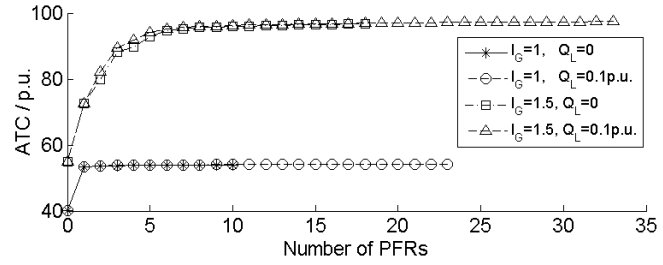

(c) PFR placement results of the IEEE 118-bus system.

Fig. 5. PFR placement for ATC enhancement. In each scenario, PFRs are added to the network until the ATC reaches 99% of the best-possible ATC for this scenario.

II when every bus of the network is equipped with a PFR.

The PFR placement results in Fig. 5 indicate that an ATC close to 99% of the best-possible ATC can be attained by placing PFRs at only 15% to 25% of the network buses. Meanwhile, in terms of ATC enhancement, the marginal benefit of adding a PFR to the power network tends to decrease as the number of PFRs available in the network increases. Therefore, it is preferable to install PFRs only at some of the critical buses to achieve a decent improvement on the network loadability without increasing the costs too much. In this light, it is desired to perform a comprehensive cost-benefit analysis, which will be part of our future work.

VI. Conclusions

The generic architecture with a load flow model of a PFR is proposed to characterize the desired functions of the PFR and to facilitate the theoretical study on power flow routing. The analysis of the load flow model indicates that a PFR is able to enlarge and decouple the control regions of its branch power flows, improving the flexibility and reliability of the power network. In addition, the PFR model is incorporated into the general OPF framework, and the PFR-OPF problem, whose objective is ATC enhancement, is formulated to assess the benefits of PFRs to the system. The proposed PFR-OPF is relaxed exactly into an SOCP problem and solved optimally. Our numerical study shows that the PFR integration to the power network can improve the loadability and reliability significantly. Future work will further explore other potential advantages of PFRs and power flow routing, such as the coordinated and dynamic control of PFRs to maintain the power balance and stability of the power network.

Acknowledgment

This work is supported in part by the Collaborative Research Fund of the Research Grants Council, Hong Kong Special Administrative Region, China, under Grant No. HKU10/CRF/10.

References

[1] "Annual energy outlook 2014 with projection to 2040," US Energy Information Adminstration, Apr. 2014.

[2] P. Nguyen, W. Kling, G. Georgiadis, M. Papatriantafilou, L. Tuan, and L. Bertling, "Distributed routing algorithms to manage power flow in agent-based active distribution network," in *Proceedings of IEEE PES IGST Europe 2010*, Oct. 2010.

[3] N. G. Hingorani, L. Gyugyi, and M. El-Hawary, *Understanding FACTS: concepts and technology of flexible AC transmission systems*. Piscataway, NJ: IEEE Press, 2000.

[4] X. She, A. Huang, and R. Burgos, "Review of solid-state transformer technologies and their application in power distribution systems," *IEEE Journal of Emerging and Selected Topics in Power Electronics*, vol. 1, no. 3, pp. 186–198, Sep. 2013.

[5] Y. Xiao, Y. H. Song, C.-C. Liu, and Y. Z. Sun, "Available transfer capability enhancement using facts devices," *IEEE Transactions on Power Systems*, vol. 18, no. 1, pp. 305–312, Feb. 2003.

[6] D. Divan and J. Sastry, "Controllable network transformers," in *Proceedings of IEEE PESC 2008*, Jun. 2008, pp. 2340–2345.

[7] R. Kandula, A. Iyer, R. Moghe, J. Hernandez, and D. Divan, "Power router for meshed systems based on a fractionally-rated back-to-back converter," *IEEE Transactions on Power Electronics*, vol. 29, no. 10, pp. 5172–5180, Oct. 2014.

[8] P. Nguyen, W. Kling, and P. Ribeiro, "Smart power router: a flexible agent-based converter interface in active distribution networks," *IEEE Transactions on Smart Grid*, vol. 2, no. 3, pp. 487–495, Sep. 2011.

[9] A. Sánchez-Squella, R. Ortega, R. Griño, and S. Malo, "Dynamic energy router," *IEEE Control Systems*, vol. 30, no. 6, pp. 72–80, Dec. 2010.

[10] X. She and A. Huang, "Solid state transformer in the future smart electrical system," in *Proceedings of IEEE PES General Meeting 2013*, Jul. 2013.

[11] J. Thomas, J. Hernandez, and S. Grijalva, "Power flow router sensitities for post-contingency corrective control," in *Proceedings of IEEE ECCE 2013*, Sep. 2013, pp. 2590–2596.

[12] J. Lavaei and S. Low, "Zero duality gap in optimal power flow problem," *IEEE Transactions on Power Systems*, vol. 27, no. 1, pp. 92–107, Feb. 2012.

[13] S. Sojoudi and J. Lavaei, "Convexification of optimal power flow problem by means of phase shifters," in *Proceeding of IEEE SmartGridComm 2013*, Oct 2013, pp. 756–761.

[14] S. Y. Hui, C. K. Lee, and F. Wu, "Electric springs – a new smart grid technology," *IEEE Transactions on Smart Grid*, vol. 3, no. 3, pp. 1552–1561, Sep. 2012.

[15] B. Zhang, A. Y. S. Lam, A. Dominguez-Garcia, and D. Tse, "Optimal distributed voltage regulation in power distribution networks," *IEEE Transactions on Power Systems*, accepted for publication, 2014.

[16] Power systems test case archive. University of Washington. [Online]. Available: http://www.ee.washington.edu/research/pstca/